Biophysical Chemistry 28 (1987) 273–281
Elsevier

BPC 01207

The lateral fluidity of erythrocyte membranes

Temperature and pressure dependence

Josef Eisinger [a] and Suzanne F. Scarlata [b]

[a] *Department of Physiology and Biophysics, Mount Sinai School of Medicine, New York, NY 10029 and* [b] *Department of Medicine, Cornell University Medical Center, New York, NY 10021, U.S.A.*

Received 17 August 1987
Accepted 19 October 1987

Membrane fluidity; Erythrocyte membrane; Lateral diffusion; High-pressure effect; Excimer; Membrane dynamics

The pressure and temperature dependence of the lateral and rotational fluidity of erythrocyte membranes was investigated by inserting the excimeric membrane probe 1′-pyrenedodecanoic acid (PDA) into the membranes of intact cells and measuring the probe excimer formation rate and the steady-state polarization of the monomer at pressures up to 2000 atm (2 kbar). At that pressure the lateral diffusivity of PDA was found to decrease by a factor of 10 and its emission anisotropy by a factor of 5 at 22° C. At atmospheric pressure, the local lateral diffusion coefficient of PDA at 2 and 33° C is 1.5 and 4.3×10^{-8} cm^2 s^{-1}, respectively. The activation energy for probe translation was found to decrease from 6 to 3 kcal M^{-1} in going from atmospheric pressure to 2 kbar, while the entropy decreased by approx. 15 cal M^{-1} K^{-1}, indicating greater lipid order at the high pressure. The experimental data are consistent with a 'free-area' model for the membrane, analogous to the free-volume model for nonassociated liquids. The lateral diffusivity of PDA was found to be proportional to the free membrane area and linear extrapolation to zero diffusivity indicates that at atmospheric pressure, the fractional free area of the erythrocyte membrane is 6%.

1. Introduction

The fluid mosaic model [1] for the basic structure of membranes implies dynamical characteristics of the molecules which constitute this quasi two-dimensional, heterogeneous fluid. Membrane lipids and proteins diffuse more or less freely in the plane of the membrane at rates which depend on the size of the molecules, on their attachment to other membrane components and on the fluidity of their environment; the last being in turn dependent on the environment's lipid composition and the local cholesterol and protein concentrations.

The fluidity of membranes has been studied using a variety of biophysical methods. The mobility of membrane polarization probes (e.g., diphenylhexatriene) has often been used to define the 'rotational fluidity' of a membrane and the model-dependent relationships between different rotational fluidity parameters have been discussed in a recent review [2]. The 'lateral fluidity' of membranes, including erythrocyte membranes [3], has usually been measured by photobleaching recovery methods, which have a characteristic diffusion distance of the order of 1 μm [4]. In the present study the lateral diffusivity of a membrane probe is derived from the rate of an intermolecular excited-state reaction (excimer formation) among the probes. The diffusion length of an excimeric probe (i.e., one capable of excimer formation) is a function of its diffusivity and the excited-state lifetime of the monomer and is of the order of a few nanometers (or lipid-lipid spacings) for pyrene-containing membrane probes. There-

Correspondence address: J. Eisinger, Department of Physiology and Biophysics, Mount Sinai School of Medicine, New York, NY 10029, U.S.A.

fore, the present method provides a measure of short-range (or local) lateral membrane fluidity [5].

The work reported here explores how variations in temperature and pressure affect the membrane fluidity of intact erythrocytes. The use of hydrostatic pressure as a thermodynamic variable makes it possible to separate changes in molecular packing from those of thermal energy. Two fluidity parameters were employed: the first provides a measure of the local lateral fluidity of the membrane for the excimer formation rate of 1'-pyrenedodecanoic acid (PDA) in the outer leaflet of the membrane and the second provides a measure of the rotational fluidity of the membrane from a determination of the steady-state emission polarization of the same probe.

The experimental results for the lateral mobility of PDA were analyzed by use of the milling-crowd model [5], in which lipids and probes in the bilayer diffuse by performing spatial exchanges with a randomly chosen neighboring molecule at a frequency which is directly proportional to the lateral diffusion coefficient, D. It will be demonstrated that the pressure dependence of D can be described by a free-volume model and that this model provides a satisfactory description of how molecular packing governs the translational mobility lipids.

2. Materials and methods

Erythrocytes were separated from freshly drawn blood provided by casual donors and were washed and suspended in 10 mM phosphate buffer containing 120 mM NaCl and 2.7 mM KCl, pH 7.4 (phosphate-buffered saline). PDA (Molecular Probes, Eugene OR) was dissolved in ethanol (after wetting with tetrahydrofuran), at a concentration of about 3 g/l. The exact concentration of the stock solution was determined spectrophotometrically, using a molar extinction coefficient in ethanol of 4.0×10^4 cm^{-1} at 342 nm. The cells were labelled at room temperature by adding microliter quantities of the stock solution to 2.5 ml of the cell suspension at a hematocrit of 0.2 while stirring. This protocol resulted in probe incorporation of efficiency greater than 95% within 10 min [6]. Molar probe ratios in the outer leaflet, x, were calculated using 2.2×10^8 for the number of lipid molecules, including cholesterol, in the outer leaflet of the red cell membrane and 1.15×10^{10} for the number of packed erythrocytes in 1 ml [7]. Samples were prepared at probe ratios ranging from 0.001 to 0.25, but only for those with x greater than 0.02 was the excimer/monomer fluorescence ratio large enough to be measured with precision, while polarization was measured in samples with low x, for which excimer formation was negligible.

All samples were diluted with phosphate-buffered saline to a maximum hematocrit of 0.002 and measured in 3-mm cuvettes for temperature studies at atmospheric pressure, or in a 1 cm round quartz bottle for high-pressure studies. High-pressure emission spectra were obtained by means of a pressure bomb and spectrofluorometer which have been described previously [8,9]. The temperature of the sample in the pressure bomb could be varied by means of a circulating bath. All spectra were corrected for a small background by subtracting those recorded for unlabelled cells. Emission polarization at high pressures was measured in a photon-counting filter fluorometer and appropriate corrections were applied for background and for the depolarization caused by the flexing of the quartz windows of the pressure bomb [8]. Steady-state emission spectra at atmospheric pressure and variable temperature were obtained by means of an SLM 4800 spectrofluorometer (SLM, Urbana, IL), using a 3 mm cuvette to reduce scattering and absorption within the sample of erythrocytes [10].

The fundamental anisotropy of PDA, r_0, was determined in a glycerol glass at $-40\,^{\circ}C$ using a 3 mm cuvette in a GREG-PC spectrofluorometer (ISS, Champaign, IL). The fundamental emission anisotropy upon excitation at 340 nm was 0.126 and 0.136 for the vibrational bands at 379 and 398 nm, respectively, with standard deviations of ± 0.003. Since the high-pressure experiments were performed with an emission filter which passed both of these wavelengths, we used the intensity-weighted average value of $r_0 = 0.130 \pm 0.006$ in calculating the depolarization factor.

3. Analysis of experiments

3.1. Lateral fluidity

Excimeric probes like PDA form excited dimers (excimers), when an excited pyrene moiety (A*) comes sufficiently close to a ground-state pyrene (A) to share its excitation energy. At room temperature, the dissociation rate of excimers is small compared to the excimer de-excitation rate [11] and one may write the following kinetic equations:

$$A^* + A \xrightarrow{K} (AA)^*$$

$$A^* \xrightarrow{k_M,\ k'_M} A + h\nu_M$$

$$(AA)^* \xrightarrow{k_E,\ k'_E} 2A + h\nu_E$$

where K is the excimer formation rate and k_M and k'_M the radiative and nonradiative de-excitation rates of the monomer, with analogous definitions for the excimer decay rates. The monomeric and excimeric quantum yields are defined by

$$\phi_M = \frac{k_M}{k_M + k'_M + K} \tag{1}$$

$$\phi_E = \frac{k_E}{k_E + k'_E} \cdot \frac{K}{k_M + k'_M + K} \tag{2}$$

At low probe concentration, $K \ll k_M + k'_M$ and ϕ_M approaches the intrinsic monomer yield, $\phi^*_M = k_M/k_M + k'_M$; and when $K \gg k_M + k'_M$, ϕ_E approaches its intrinsic value, $\phi^*_E = k_E/k_E + k'_E$. It is then readily seen from eqs. 1 and 2 that at a concentration, x,

$$\frac{\phi_E(x)}{\phi_M(x)} = \frac{\phi^*_E}{\phi^*_M} K\tau_M \equiv CK\tau_M \tag{3}$$

where

$$\tau_M = (k_M + k'_M)^{-1} \tag{4}$$

is the monomer lifetime and C a constant of order unity. The excimer formation rate is a function of the probe concentration, expressed as the probe/lipid molar ratio, x, as well as of their lateral diffusivity and can be expressed in terms of the rate, f, at which probes and lipids change places,

$$K(x) = f/n(x) \tag{5}$$

where $n(x)$ is the average number of random spatial exchanges between probes and lipids, which leads to the formation of an excimer. $n(x)$ is therefore a function of p_E, the probability of excimer formation between nearest neighbors, as well as x. Values of $n\ (p_E,\ x)$ have been obtained by means of computer simulations based on the milling-crowd model [5]. The exchange frequency, f, is determined by fitting the x dependence of the monomer yields, normalized at low concentrations, to the following equation derived from eqs. 1, 4 and 5:

$$\frac{\phi_M(x)}{\phi^*_M} = \left[1 + \frac{f\tau_M}{n(p_E,\ x)}\right]^{-1} \tag{6}$$

In two dimensions the lateral diffusion coefficient, D, can be expressed in terms of the frequency at which a probe takes random steps of length L, the average lipid-lipid spacing in the membrane [12]:

$$D = fL^2/4 \tag{7}$$

so that from eqs. 3, 4 and 7, the excimer/monomer intensity ratio, $\Gamma(x)$ is

$$\frac{\phi_E(x)}{\phi_M(x)} \equiv \Gamma(x) = \frac{4CD\tau_M}{L^2 n(p_E,\ x)} \tag{8}$$

τ_M for pyrene decreases by about 10% when the pressure, p, is raised from atmospheric pressure (1 bar) to 2000 bar (2 kbar), both in micelles [13] and as a solute in toluene [14]. L has an even weaker dependence on p (cf. fig. 8). Therefore, the pressure dependence of D in terms of the ratio $\Gamma(x)$ is according to eq. 8, at least approximately,

$$D(p)/D(1) = \Gamma(p)/\Gamma(1) \tag{9}$$

where $\Gamma(1)$ and $D(1)$ are the values of $\Gamma(p)$ and $D(p)$ at atmospheric pressure.

More generally, it can be seen from eq. 8 that if the membrane probe concentration x remains constant, the diffusivity at pressure p_1 and temperature T_1 is related to that at p_2 and T_2 by the

following equation

$$\frac{D(p_1, T_1)}{D(p_2, T_2)} = \frac{\Gamma(p_1, T_1)}{\Gamma(p_2, T_2)} \cdot \frac{\tau_M(p_2, T_2)}{\tau_M(p_1, T_1)} \qquad (10)$$

where the monomer lifetimes on the right-hand side are determined experimentally under the stated conditions. Note that eq. 10 is independent of $n(x)$ and, therefore, of any specific model of membrane dynamics.

The intensity ratio Γ is, moreover, considerably less sensitive to scattering and absorption within the sample than the fluorescence intensity itself [15]. This is an important consideration in high-pressure experiments with erythrocytes, since the cells in the cuvette settle in the course of the experiment.

3.2. Rotational fluidity

The relationship between the rotational rate of an isotropically rotating molecule and the steady-state polarization of the fluorescence it emits, is given by the Perrin equation [16]:

$$\langle r \rangle = r_0(1 + \tau/\tau_R)^{-1} \qquad (11)$$

Here $\langle r \rangle$ and r_0 are the molecule's steady-state and fundamental anisotropy, respectively, τ the lifetime of its excited state and τ_R its rotational correlation time. The pyrene moiety of PDA in the lipid bilayer is, on the other hand, in an anisotropic environment with its rotational mobility constrained. Under these conditions, the fluorophore's emission anisotropy does not decay to zero after a long time (t), as it does for isotropic rotators, but approaches a limiting value, r_∞ [17,18]. If the approach to r_∞ is monoexponential, it may be represented by

$$r(t) = (r_0 - r_\infty)\exp(-t/\tau_R) + r_\infty \qquad (12)$$

By weighting $r(t)$ with the emission intensity and integrating,

$$\langle r \rangle = (r_0 - r_\infty)\tau_R/(\tau_R + \tau) + r_\infty \qquad (13)$$

where τ is the excited-state lifetime [19]. Upon rearrangement of this equation one obtains

$$r_\infty = \langle r \rangle - (r_0 - \langle r \rangle)(\tau_R/\tau) \qquad (14)$$

A complete study of a probe's rotation clearly requires the experimental determination of its anisotropy decay but the present work reports only steady-state emission polarization. It is then useful to write eq. 14 in terms of the steady-state depolarization factor, $\langle d \rangle = \langle r \rangle / r_0$, and the limiting depolarization factor, $d_\infty = r_\infty / r_0$:

$$d_\infty = \langle d \rangle - (1 - \langle d \rangle)(\tau_R/\tau) \qquad (15)$$

This equation shows how the measured average depolarization depends both on the limiting depolarization and on the rotational rate of the probe. The interdependence of the latter two parameters is displayed graphically in fig. 1, in which the family of lines represent the range of d_∞ and τ_R/τ values which are consistent with the experimental $\langle d \rangle$ values.

At increasing pressure, the free volume of the membrane shrinks and d_∞ increases and approaches unity, as was indeed observed in several model systems [20], but a concomitant increase in τ_R cannot be ruled out on the basis of steady-state polarization experiments alone.

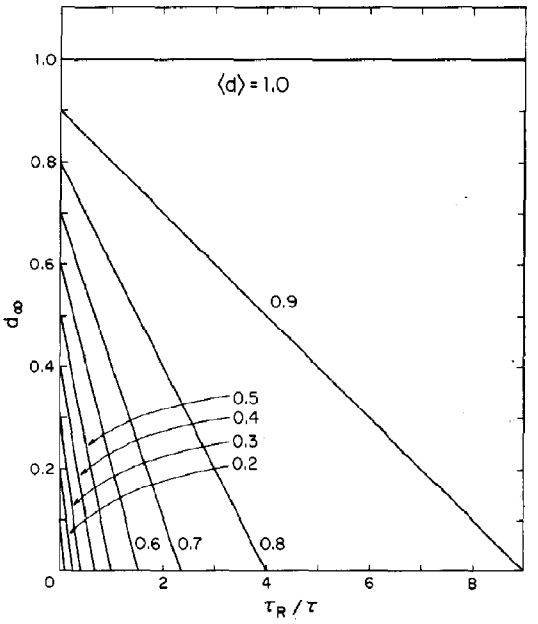

Fig. 1. The family of straight lines show the ranges of limiting depolarization factors, d_∞, and rotational correlation times, τ_R, which are consistent with particular values of the steady-state depolarization, $\langle d \rangle$, according to eq. 14.

4. Experimental results

Emission spectra of PDA in the membranes of intact erythrocytes were measured at pressures from 1 bar to 2 kbar and examples of spectra normalized, to the peak of the monomer emission intensity, are shown in fig. 2. Upon returning to atmospheric pressure the excimer/monomer intensity ratios were found to be reversible and the erythrocytes were found to be morphologically unchanged when examined microscopically, with no evidence of hemolysis.

The pressure dependence of the lateral diffusion coefficient, D, was determined by use of eq. 9 from the excimer/monomer ratios (I_E/I_M) measured at 480 and 377 nm for four samples with probe ratios between 0.01 and 0.25. According to the milling-crowd model and eq. 8, the product $[I_E(x)/I_M(x)]n(p_E, x)$ is independent of the probe ratio. This was found to be the case at all pressures up to 2 kbar. Since τ_M is almost independent of pressure [14,15], the variation of D with pressure was obtained by use of eq. 9 and the results (averaged over three samples with $x =$ 0.042, 0.13 and 0.25) are shown in fig. 3.

The probe ratio dependence of the normalized PDA monomer yield, $J_M(x)/J_M^*$, at three temperatures is shown in fig. 4 along with curves fitted to the data according to eq. 6. The fit of the data to the theoretical curves is good except in cells with probe/lipid ratios greater than 0.1, in which the membrane's dynamic properties may have been altered, x_0, the probe ratio for which the excimer production rate equals the monomer decay rate, is found to be 0.16, 0.13 and 0.12 at 2, 20 and 33°C, respectively. x_0 is a good empirical indicator of local lateral fluidity (see fig. 4).

Absolute values of the diffusivity of PDA may be calculated from the data of fig. 4 by employing the milling-crowd model. From the fitted curves or the corresponding x_0 values, the exchange frequency, f, was determined to be 0.9, 1.8 and

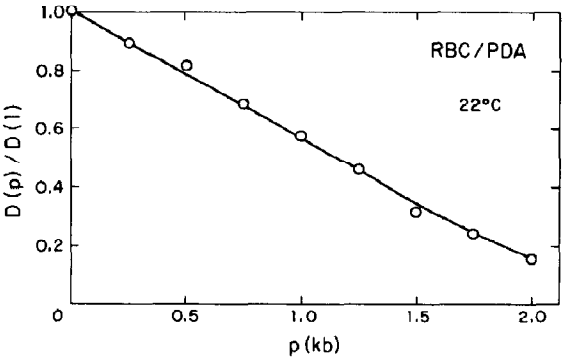

Fig. 3. Pressure dependence of the lateral diffusion coefficient $D(p)$ normalized to its value at atmospheric pressure, $D(1)$, at 22°C.

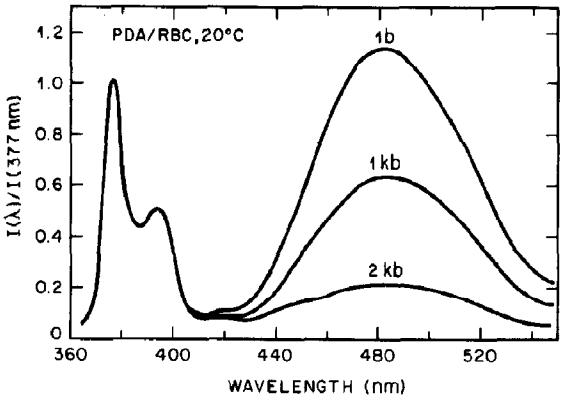

Fig. 2. Uncorrected emission spectra of 1'-pyrenedodecanoic acid in the membrane of intact erythrocytes at atmospheric pressure (1 bar, 1b) and at hydrostatic pressures of 1 and 2 kbar (1kb, 2kb). The spectra are normalized to the monomer peak intensity at 377 nm and were excited at 340 nm.

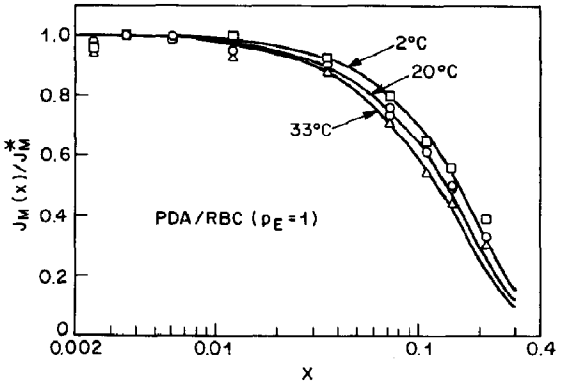

Fig. 4. Dependence of the normalized monomer yield, $J_M(x)/J^*$, on the probe ratio, x, measured at three temperatures. The yields are defined by $J_M(x) = I(x)/x$, with J_M^* being the limiting yield at low x and $I(x)$ being the fluorescence intensity.

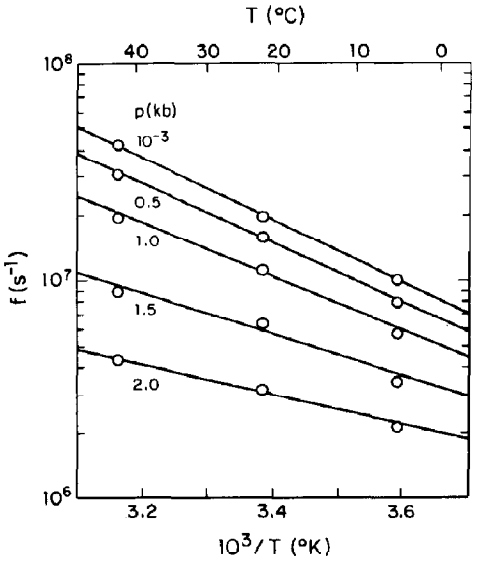

Fig. 5. Pressure and temperature dependence of the effective probe-lipid spatial exchange frequency, f. The values of f were obtained from computer simulations for $n(p_E, x)$ according to the milling-crowd model with p_E, the excimer formation probability between nearest neighbor probes, taken as unity. They therefore represent lower limits of f, as explained in the text.

2.7×10^8 s^{-1} at 2, 20 and 33°C, respectively, in good agreement with the jump frequency of excimeric probes in erythrocyte ghosts and extracted

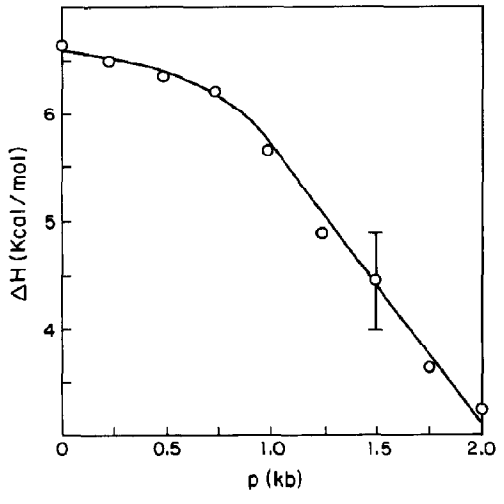

Fig. 6. Pressure dependence of the activation energy, ΔH, for probe translation obtained from the slopes of the Arrhenius plots shown in fig. 4.

lipids [21]. The average monomer lifetimes at these temperatures, which are required for solving eq. 6, were estimated to be 94, 74 and 65 ns from the relative fluorescence yields at different temperatures and the measured τ_M at 20°C [5]. By use of eq. 7 with $L = 0.8$ nm, the lateral diffusion coefficient of PDA is found to be 1.5, 2.9 and 4.3×10^{-8} cm^2 s^{-1} at 2, 20 and 33°C, respectively.

By combining the high-pressure data obtained at three temperatures (fig. 3) with the atmospheric pressure diffusivity values obtained above, one obtains the Arrhenius plots of fig. 5. Their slopes were used to determine the activation energy, ΔH, of the probe-lipid spatial exchange, whose pressure dependence is shown in fig. 6. ΔH is seen to decrease from a value of 6 ± 1 kcal M^{-1} at atmospheric pressure to 3 ± 1 kcal M^{-1} at 2 kbar.

The entropy change at high pressure is obtained from the intercepts of the Arrhenius plots with the assumption that the preexponential factor remains unchanged. In raising the pressure from 1 to 2 kbar, the entropy is found to decrease by 15 cal M^{-1} K^{-1}, reflecting greater order of the probe-lipid system at high pressure.

It is of interest to compare this value to the entropy change, ΔS, of the three-dimensional liquid, upon the application of pressure, Δp. At a constant temperature,

$$\Delta S = V_m(dV/dT)\Delta p \qquad (16)$$

where V_M and dV/dT are the molar volume and coefficient of volume expansion of the liquid, respectively. For olive oil, dV/dT is 0.0007 K^{-1} and V_M about 300 ml M^{-1}; the entropy change upon the application of 2 kbar is therefore about 10 cal M^{-1} K^{-1}.

The rotational mobility of the fluorophore of PDA was estimated from its steady-state emission polarization. To avoid complications in analyzing the data, all polarization experiments employed samples with probe ratios of 1% or less, for which excimer production rates are negligible. The pressure dependence of the steady-state anisotropy measured at three temperatures is shown in fig. 7. The corresponding values of the steady-state depolarization factor, $\langle d \rangle$, were obtained with $r_0 = 0.130$ and are shown in the same figure (cf. section 2).

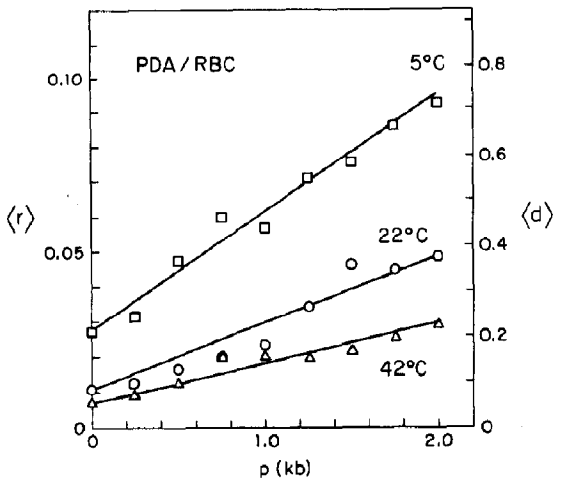

Fig. 7. Pressure dependence of the steady-state emission anisotropy of PDA in erythrocyte membranes at three temperatures. The experimental error in $\langle r \rangle$ is ± 0.004 and the values of $\langle d \rangle$ with $r_0 = 0.130$ are shown on the right-hand side.

If the rotational mobility of the pyrene moiety can be approximated by a single rotational correlation time, one may use eq. 15 and fig. 1 to interpret the results of fig. 7. For example, the depolarization at atmospheric pressure and 5 °C, $\langle d \rangle = 0.2$, implies that τ_R/τ is less than 0.5 (or τ_R is less than about 40 ns) and that d_∞ is less than 0.2 (or r_∞ is less than 0.26). Quite generally, eq. 14 states that for any particular $\langle r \rangle$, the larger is r_∞, the smaller is the corresponding τ_R.

5. Discussion

A reduction in the excimer/monomer ratio of pyrene with pressure (measured at an undefined probe concentration), similar in magnitude to that reported here, has been observed in erythrocyte ghosts and vesicles made from ghost lipids [22]. The slight change in slope of the pyrene excimer/monomer ratio with pressure, which was suggested to represent a phase transition in ghost membranes [22], may have other causes, although pressure-induced phase transitions do occur in homogeneous model systems [23,24]. No evidence for phase transitions was found in the present study.

The experiments reported here can be discussed in terms of a free-volume model which has been successful for isotropic fluids. From the experimental values of viscosity and specific volume of many nonassociated liquids measured over a wide temperature range, Batschinski discovered a simple relationship between the liquid's free volume and its dynamic properties [25,26]. It states that the fluidity (F), or inverse viscosity, is proportional to its free volume, defined as the difference between its molar volume (V) and its limiting volume (Ω) which can be identified with the volume occupied by the molecules themselves (van der Waals volume).

$$F = \text{constant}(V - \Omega) \tag{17}$$

This study provides an opportunity to test the applicability of this simple relationship to a membrane, i.e., to a heterogeneous, quasi-two-dimensional liquid.

From the pressure dependence of the diffusivity of PDA in the erythrocyte membrane (cf. fig. 3) one may derive the dependence of D on the membrane area by assuming that the compressed red cell retains its shape while reducing its volume according to the compressibility (c) of its cytoplasm. At a pressure p, the cell's volume is therefore

$$v(p) = v(1)(1 - cp) \tag{18}$$

while the area of its membrane at pressure p, $A(p)$, is

$$A(p) = A(1)(1 - cp)^{2/3} \tag{19}$$

where $A(1)$ is the membrane area at $p = 1$ bar. Here c is the compressibility of the cytoplasm, a 34% hemoglobin solution. Since proteins have a negligible compressibility [27], c is estimated to be $(0.66)c_w$, where c_w is the (pressure-dependent) compressibility of water (about 0.04 kbar^{-1}) [28]. From eq. 18 and the data of fig. 3 one may the derive the dependence of D on membrane area, which is shown in fig. 8. If the linear dependence of $D(p)/D(1)$ on area is extrapolated to vanishing diffusivity, it may be described by the following relationship

$$\frac{D(p)}{D(1)} = \frac{A(p) - A_m}{A(1) - A_m} \tag{20}$$

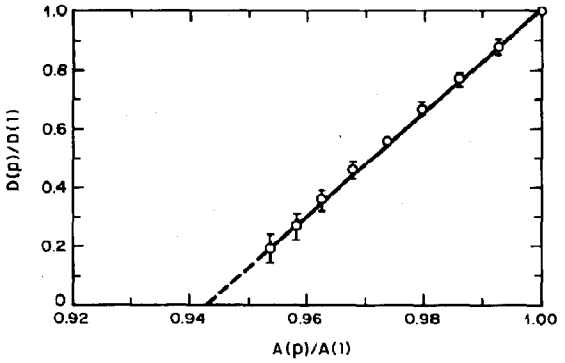

Fig. 8. Dependence of the relative lateral diffusivity of PDA in the erythrocyte membrane as a function of the relative membrane area of the cell. A linear extrapolation of the data according to eq. 21 suggest that the fractional free area of the membrane is approx. 6%.

or

$$D(p) = \text{constant}[A(p) - A_m] \qquad (21)$$

where A_m is identified with the total area occupied by the molecular components of the membrane. It is the area at which the lateral fluidity of the membrane vanishes.

The physical meaning of eq. 21 is simply that lipids in the membrane slide past each other (i.e., diffuse) at a rate which is proportional to the membrane's free area, i.e., the area not occupied by membrane molecules. In the limit of high pressures, the free area vanishes and the membrane resembles a solid with zero fluidity. Our data suggest that the minimum area of the red cell membrane at sufficiently high pressures is $A_m = (0.94)A(1)$, or equivalently, that the membrane's fractional free area at atmospheric pressure is approx. 6%. A lateral membrane compressibility of this magnitude is consistent with that of phosphatidylcholine/cholesterol multilayers, measured in a neutron diffraction experiment over the same pressure range [29]. The same study reported a 4% increase in bilayer thickness, which is though to be related to greater ordering at high pressure.

The area of human erythrocytes, $A(1)$, is 143 μm^2 [30] and the number of lipid molecules, including cholesterol, in the outer leaflet of the membrane is estimated to be 2.2×10^8 [7]. If the membrane proteins are assumed to occupy 30% of the membrane's area [31] and are incompressible [27], the area occupied by a lipid molecule is approx. 0.45 nm^2, corresponding to an average separation of 0.67 nm and an average free separation of 3% or about 0.02 nm.

Because of the intimate connection between the free area and dynamic properties of the membrane, the determination of the pressure dependence of a membrane's fluidity provides a useful method of characterizing cell membranes. At the highest pressures employed here some cell functions are impaired [32] and erythrocyte ghosts shed some cytoskeletal proteins [33], but it is seen that considerably lower pressures, say, tens of atmospheres, are sufficient to measure the pressure coefficient of the probe's lateral diffusivity with accuracy. The initial pressure coefficient of D, defined as

$$\alpha \equiv (dD/dp)_{p=1}/D(1) \qquad (22)$$

is, according to fig. 3, 0.42 $kbar^{-1}$ for normal erythrocytes at room temperature.

In summary, the diffusivity of PDA in the red cell membrane which is an indicator of the membrane's lateral fluidity was found to decrease by an order of magnitude at a pressure of 2 kbar. Over the same pressure range the activation energy for probe motion decreases by about a factor of two and the free area of the membrane is reduced by 6%.

How are these findings related and what dynamic model for the membrane is suggested by them? The drastic reduction in free area shown in fig. 7 is the reason for the observed increase in PDA anisotropy (cf. figs. 1 and 6). The loss of free area hinders the translation of probes and phospholipids in the bilayer and is the reason for the reduced local diffusivity of the probes. High pressure also leads to an increase of order in the probe-lipid structure which is reflected in a lowering in the enthalpy of probe translation and a decrease in entropy. According to the vacancy theory of molecular transport, the lateral diffusivity of a molecule is determined by the rate at which suitable vacancies are created in the membrane [34]. Our results show that at high pressures, the vacancies created by thermal motion are on average smaller, but because the probes and lipids

are better aligned, the energy barrier to occupying them is reduced.

Acknowledgements

We are grateful to J. Flores for technical assistance and to G. Weber, J.B.A. Ross and M. Sassaroli for illuminating discussions. We also thank G. Weber, C.A. Royer and J. de Silva for making their high-pressure instrumentation available to us.

References

1 S.J. Singer and G.L. Nicolson, Science 175 (1972) 720.
2 W. van der Meer, H. Pottel, H. Herreman, M. Ameloot, H. Hendrickx and H. Schroeder, Biophys. J. 46 (1986) 515.
3 J.A. Bloom and W.W. Webb, Biophys. J. 42 (1983) 295
4 D. Koppel, D. Axelrod, J. Schlessinger, E. Elson and W. Webb, Biophys. J. 16 (1976) 1315.
5 J. Eisinger, J. Flores and W.P. Petersen, Biophys. J. 49 (1986) 987.
6 J. Eisinger and J. Flores, Biophys. J. 48 (1985) 77.
7 C.C. Sweeley and G. Dawson, in: Red cell membrane, eds. G.A. Jamieson and T.J. Greenwell (Lippincott, Philadelphia, 1969) p. 173.
8 C.A. Royer, Ph.D. Thesis, University of Illinois, Urbana, IL (1985).
9 A.A. Paladini and G. Weber, Rev. Sci. Instrum. 52 (1981) 419.
10 J. Eisinger and J. Flores, Anal. Biochem. 94 (1979) 15.
11 T. Förster and H.-P. Seidel, Z. Phys. Chem. N.F. 45 (1965) 58.
12 H.C. Berg, Random walks in biology (Princeton University Press, Princeton, NJ, 1983).
13 N.J. Turro, M. Okamoto and P.-L. Kuo, J. Phys. Chem. 91 (1987) 1819.
14 P.C. Johnson and H.E. Offen, J. Chem. Phys. 56 (1972) 1638.
15 J. Eisinger and J. Flores, Biophys. J. 48 (1985) 77.
16 F. Perrin, J. Phys. Radium 5 (1934) 497.
17 R.E. Dale, L.A. Chen and L. Brand, J. Biol. Chem. 252 (1977) 7500.
18 B.W. van der Meer, R.P. van Hoeven and W.J. Blitterswijk, Biochim. Biophys. Acta 854 (1986) 38.
19 M.P. Heyn, FEBS Lett. 108 (1979) 359.
20 J.R. Lakowicz and R.B. Thompson, Biochim. Biophys. Acta 732 (1983) 359.
21 H.-J. Galla and J. Luisetti, Biochim. Biophys. Acta 596 (1980) 108.
22 M. Flamm, T. Okubo, N.J. Turro and D. Schachter, Biochim. Biophys. Acta 687 (1982) 101.
23 N. Liu and R.L. Kay, Biochemistry 16 (1977) 3484.
24 P.L.-G. Chong, and G. Weber, Biochemistry 22 (1983) 5544.
25 A. Batschinski, Z. Phys. Chem. 84 (1913) 643.
26 E.C. and P.W. Kinney, J. Appl. Phys. 11 (1940) 192.
27 B. Gavish, E. Gratton and C.J. Hardy, Proc. Natl. Acad. Sci. U.S.A. 80 (1983) 750.
28 G.S. Kell, in Water. A comprehensive treatise, ed. F. Frank (Plenum Press, New York, 1972) p. 385.
29 L.F. Braganza and D.L. Worcester, Biochemistry 25 (1986) 7484.
30 D. Branton and D.W. Deamer, in: Membrane structure (Springer Verlag, New York, 1972) p. 4.
31 J. Eisinger, in: Fluorescent biomolecules: methodologies and applications, eds. D.M. Jameson and G.D. Reinhart (Plenum Press, New York, 1988) in the press.
32 A.G. Macdonald, Phil. Trans. R. Soc. Lond. B304 (1984) 47.
33 M. Deckman, R. Haimowitz and M. Shinitzky, Biochim. Biophys. Acta 821 (1985) 334.
34 M.H. Cohen and D. Turnbull, J. Chem. Phys. 31 (1959) 1164.